

Testing Echo Amplitude Changes in relation to an Ultrasonic Beam Angle of Incidence at a Flat-Bottomed Reflector

Abstract: The article presents issues related to ultrasonic testing of welded joints and includes results of tests dedicated to the detectability of flat discontinuities depending on their orientation in relation to the ultrasonic beam axis. In the tests, flat discontinuities were constituted by circular flat-bottomed reflectors of DGS-45° standard having a diameter $D_{DSR}=2$ mm. The tests were performed using a Phased Array transducer and a defectoscope with a Phased Array imaging package enabling the determination of echo amplitude for various beam insertion angle values. As a result, it was possible to obtain the characteristics of a decibel echo drop depending on the beam angle of incidence on the flat-bottomed reflector in a range from the optimum to a disadvantageous value. The article includes a diagram “distance – amplification - beam angle of incidence on the reflector” enabling the determination of an echo amplitude drop accompanying the changes of angles at which the beam strikes a discontinuity by 5°, 10° and 15°.

Keywords: ultrasonic testing, welded joints, ultrasonic beam angle, echo amplitude changes

DOI: [10.17729/ebis.2015.4/5](https://doi.org/10.17729/ebis.2015.4/5)

Introduction

When performing ultrasonic tests (UT) for welded joint quality control it is necessary to take into consideration a number of factors affecting both the possibility of performing tests and the subsequent assessment of their accuracy. The first group of factors is associated, among others, with providing access to a search surface required by standards and the appropriate width of a head movement zone [3, 4]. The second group of factors includes, among other things, the proper selection of heads for ultrasonic tests (frequency, size of transducer, head

angle). These factors significantly affect the detectability of flat discontinuities such as cracks and incomplete fusions, particularly dangerous from the crack mechanics point of view. Previous tests revealed that the detection of unfavourably oriented flat discontinuities may be difficult using conventional UT, even when two beam insertion angles are used. This issue was addressed in the publication [2] describing tests confirming the significant impact of discontinuity orientation on echo amplitude for three various angles at which the beam strikes the discontinuity. This inspired an attempt to determine echo

mgr inż. Rafał Kaczmarek (MSc Eng., scholarship holder within the project entitled “DoktoRIS – Scholarship Programme for innovative Silesia, co-financed by the European Union within the European Social Fund) – Częstochowa University of Technology; Welding Department

amplitude drop characteristics in relation to flat discontinuities and their orientation measured using angle γ at which the beam strikes a discontinuity. The publication [1] presented tests where the discontinuity was an infinite reflector in the form of a skew surface of the DGS-45° standard. This article is the continuation of the previously addressed subject and presents results and analysis of tests involving circular flat-bottomed reflectors (DSR) having a diameter $D_{DSR}=2$ mm. Such a solution enabled the obtainment of beam reflection conditions close to conditions present while detecting slight flat discontinuities in welded joints.

The primary criterion taken into consideration when assessing UT indications of welded joints is echo amplitude in relation to a specified reference level. The assessment consists in comparing such amplitude with the required acceptance level. Therefore, it is of great importance to obtain the maximum echo amplitude from a discontinuity. The objective of this publication was to demonstrate how this amplitude decreases if the angle at which the beam strikes a discontinuity is not optimum. Such a situation takes place, among others, in conventional ultrasonic tests when the orientation of a flat discontinuity in relation to the applied beam insertion angle slightly or significantly differs from the favourable value.

Testing methodology

The tests involved the use of an Olympus Epoch 1000i ultrasonic defectoscope with a Phased Array imaging package. The defectoscope was equipped with a 16-element 5L16-A10P head having a frequency of 5 MHz and an active aperture of 9.6 mm with a SA10P-N55S wedge. The calibration of zero (follow-up) and of sensitivity was made on radius R100 of standard no. 1. The test involved the use of a beam without focusing.

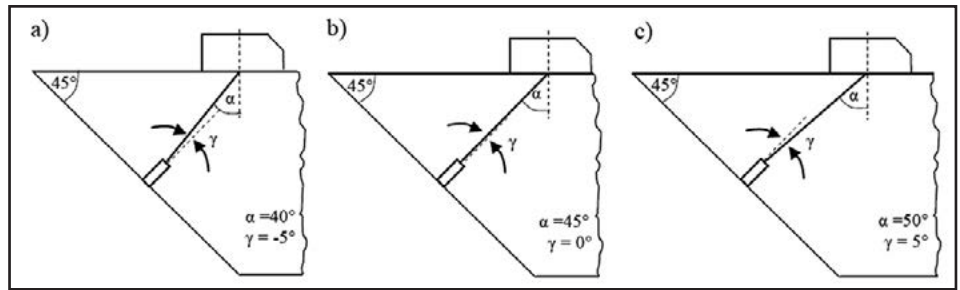


Fig. 1. Diagram of changes of angle γ at which the beam struck a discontinuity with the direct reflection of a beam off the reflector for beams insertion angles of $\alpha=40^\circ$, $\alpha=45^\circ$ and $\alpha=50^\circ$

The specimen used in the tests was a standard DGS 7x Φ 2x10-45°, whereas flat discontinuities had the form of seven circular flat-bottomed reflectors having a diameter of $D_{DSR}=2$ mm. By changing a beam insertion angle α , it was possible to obtain echo from reflectors for various angles γ at which the beam struck the discontinuity. This enabled the recording of the gain V for which the discontinuity echo reached 80% of the full screen height (FSH) for various ultrasonic beam axis orientations in relation to the reflector. As can be easily noticed, the most favourable orientation ($\gamma=0^\circ$) was where the beam insertion angle amounted to

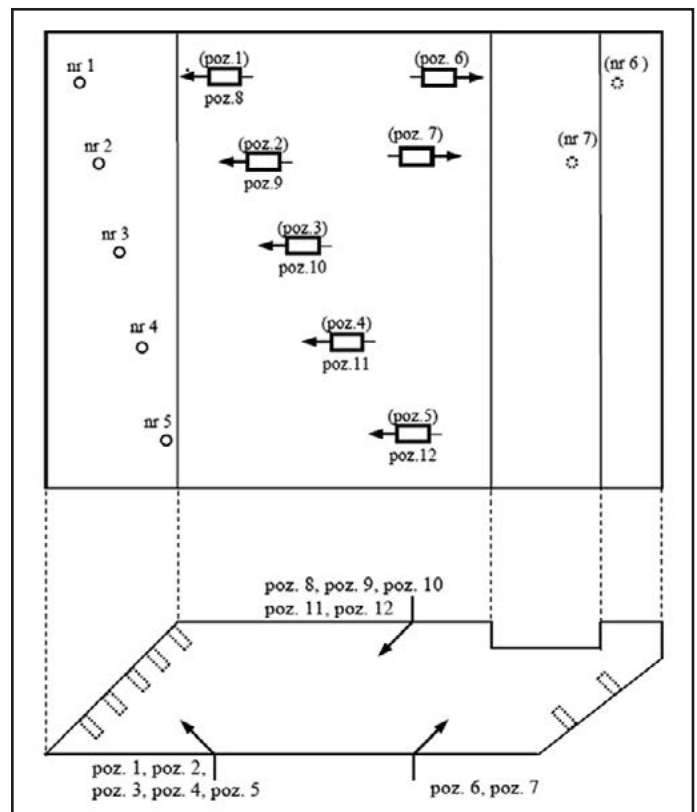


Fig. 2. Numbering of flat-bottomed apertures (1÷7) and head positions (1÷12) during testing from both DGS standard surfaces

$\alpha=45^\circ$ (Fig. 1). Figure 2 presents the numbering of flat-bottomed apertures and head positions for testing from both DGS standard surfaces. For head position no. 1, the test was performed with beam insertion angles α restricted in the range of $40-70^\circ$ with an angle changing each 0.5° . This approach enabled the recording of echo for sixty various angles at which the beam struck a discontinuity. In turn, for head position numbered 5-12, beam insertion angles α were restricted in the range of $40-60^\circ$, with an angle changing each 1° (for some positions the lack of place on the DGS standard precluded the obtainment of echo for angles close to 60°).

It should be noted that, in fact, each head position (1-12) is composed of several dozen sub-positions. For instance, when recording gain V from position no. 5 for each beam insertion angle α , the test was performed from positions designated by a position number and an angle value, e.g. pos. 5/40°, pos. 5/45°, pos. 5/50° (Fig. 3a) etc. Therefore, for a given head position and various angles α , the beam path is not constant but increases gradually along with a growing angle α , simultaneously affecting the drop of echo amplitude from the reflector. This is due to the fact that an increase in a path length is connected with greater acoustic pressure losses resulting from ultrasonic beam damping and divergence (phenomenon taking place outside the field close to the head, in accordance with the DGS curve drop). The greater the beam insertion angle α , the greater the length beam path S and the greater the amplitude drop resulting from beam damping and divergence. This fact must be taken into consideration when analysing results. Table 1 presents the lengths of beam path S for selected values of beam insertion angle α . It can be seen that for a given head position

the difference between the path length for the minimum $\alpha=40^\circ$ and maximum $\alpha=60^\circ$ angles does not exceed 40 mm.

Test Results and Analysis

Figure 4 presents a diagram with test results obtained for head position no. 1, beam insertion angle restricted in the range of $\alpha=40-70^\circ$ and a beam path length value restricted in the range of $S_1=15.41-32.8\text{mm}$, corresponding to the beam insertion angle. The x-axis represents the beam insertion angle α , whereas the y-axis represents gain V , for which echo amounted to 80% of the full screen height (FSH). The values on the vertical axis were placed in a reversed (decreasing) sequence, analogously as in distance-gain-size (DGS) diagrams. In this manner, the curve maximum in the diagram corresponded to the maximum echo amplitude requiring the lowest gain V necessary to obtain echo of 80% FSH. In addition, Table 2 presents gain V values and their

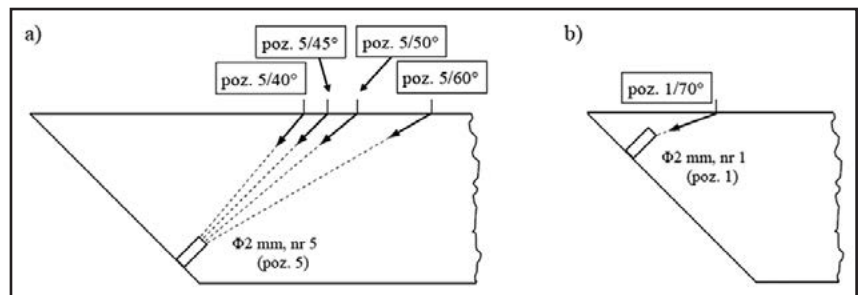


Fig. 3. Diagram of changes of head positions and of path lengths for various beam insertion angles α

Table 1. Length of beam path S for individual head positions and beam insertion angles α of $40^\circ, 45^\circ, 50^\circ, 55^\circ$ and 60°

Head position	Beam insertion angle $\alpha, ^\circ$				
	40°	45°	50°	55°	60°
	Beam path S , mm				
Position 1	15.41	16.73	18.70	20.68	25.48
Position 5	41.83	45.91	50.45	56.72	64.53
Position 6	44.55	53.24	58.14	65.08	71.65
Position 7	57.15	60.55	66.68	74.66	-
Position 8	70.78	76.31	82.80	92.67	105.81
Position 9	77.93	83.35	91.28	100.67	115.25
Position 10	84.47	91.30	99.34	110.94	-
Position 11	91.85	98.54	107.0	118.39	-
Position 12	98.45	106.21	115.27	125.31	-

corresponding path S values for selected beam insertion angles α . As was expected, the highest echo amplitude was obtained for a beam insertion angle of $\alpha=45^\circ$ (gain $V=23$ dB).

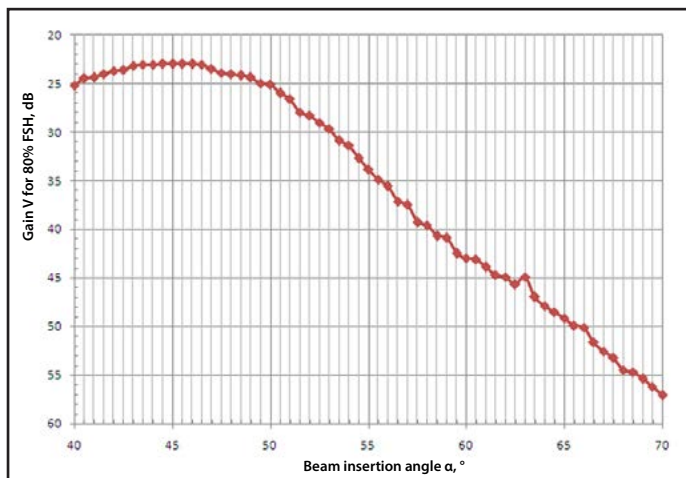


Fig. 4. Diagram of gain V in relation to beam insertion angle α for head position no. 1 and beam path in the material restricted in the range of $S_1=15.41-32.8$ mm

Table 2. Test results for head position no. 1 and selected beam insertion angles α

	Beam insertion angle α , °						
	40°	45°	50°	55°	60°	65°	70°
	Angle at which the beam strikes the reflector γ °						
Beam path S, mm	-5°	0°	5°	10°	15°	20°	25°
Gain V for 80% FSH, dB	15.41	16.73	18.70	20.68	25.48	29.57	32.80
	25.2	23.0	25.1	33.8	43.0	49.2	57.1

The angle corresponds to such reflector orientation in relation to the ultrasonic beam axis where the angle between the beam axis and the normal to the reflector surface is optimum and amounts to $\gamma=0^\circ$ (Fig. 1b). In such a situation the beam strikes the surface of a flat-bottomed aperture perpendicularly. An amplitude drop along with the change of angle of incidence by 5° - both towards positive and negative values of angle γ - is equal in both cases and amounts to $\Delta V=2$ dB. In turn, the further increasing of angle α within the range of $50^\circ-70^\circ$ results in the approximately linear amplitude change revealing a significantly greater drop. It should be noted that for the considered range of angle α , beam path S increased from 18.7 mm to

32.8 mm, which demonstrated that the reflector was in the field close to the head.

The characteristic obtained for angle α values close to 70° should not be rigorously treated as the dependence of echo amplitude drop related to the flat-bottomed aperture surface. This can be ascribed to the fact that for high angle α values, echo came not from the reflector surface, but from its edge directed towards the beam axis (pos. 1/70°, Fig. 3b). This fact was clearly visible on S-scan imaging, where, for angle α values close to 70° , an initially visible wide indication obtained from the reflector surface transformed into a point indication from the edge. This justifies the supposition that for these values of angle α , the drop in the amplitude of echo from the surface (ignoring the echo from the surface edge) could be even higher than the value obtained in the test.

For this reason, in the tests of the remaining positions (5÷12), echo was recorded within the range of beam insertion angle $\alpha=40^\circ-60^\circ$, ignoring the range of $60^\circ-70^\circ$.

Figure 5 presents the test results related to the remaining positions of the head (pos. 5÷12). As can be seen, the characteristic of echo amplitude drop is similar for all the positions,

and thus, it does not reveal greater differences for increased distance between the head and subsequent flat-bottomed apertures, resulting in the beam path change from $S_1/45^\circ=16.73$ mm to $S_{12}/45^\circ=106.21$ mm (path values for angle $\alpha=45^\circ$). While comparing individual curves, it was only possible to observe that their maxima tended to shift slightly towards lower angle α values (for position 1 the maximum was at an angle of 45° , for position 6 at an angle of 44° , whereas for position 12 at an angle of 43°). In turn, locally present slight curve knees could result from an inaccurate measurement for a given measurement point (position and angle α , e.g. pos. 6/49°). This was due to the fact that it is very difficult to obtain the maximum echo

from a small-diameter flat-bottomed aperture particularly for high values of angle α . In such situations it is necessary to precisely direct the head towards the reflector in three degrees of freedom (front-rear, left-right, head rotation).

The gradual shift of individual curves towards greater gain (downwards) results from the necessity of compensating beam damping and divergence-related losses, directly connected with increasing beam path lengths for successive positions (from pos. 1 to 12). This shift results from the DGS curve of the head and is of no significance in relation to the subject of the analysis performed.

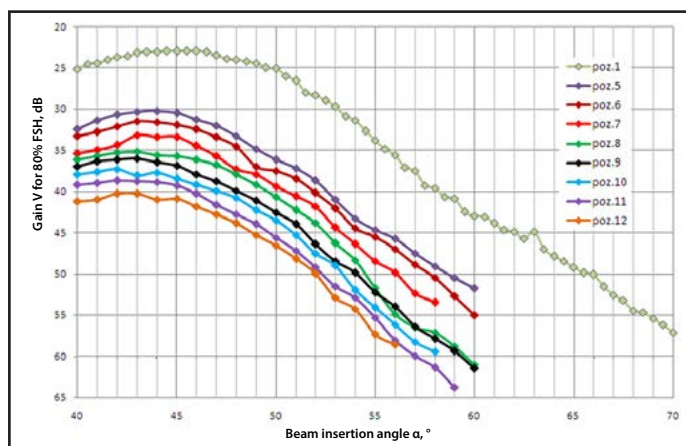


Fig. 5. Diagram of gain V in relation to beam insertion angle α for head position no. 1 and 5-12

However, it should be noted that changes of echo amplitude in the function of angle α for individual curves presented in Figure 5 result from two factors:

- change of angle γ at which the beam strikes the reflector due to the change of beam insertion angle,
- beam path length changes within one head position (one curve) and individual beam insertion angles – the greater the beam insertion angle, the longer the path S, and at the same time, the greater the acoustic pressure drop related to beam damping and divergence.

In order to separate the effect of the first factor only, it was necessary to make the diagram “distance S – gain V - angle γ at which the beam strikes the reflector”, or a DGA diagram (Fig. 6). The characteristic was made up of gain V results

from positions 5 through 12 and beam insertion angles of $\alpha=45^\circ, 50^\circ, 55^\circ$ and 60° corresponding to angles of incidence at the reflector of $\gamma=0^\circ, 5^\circ, 10^\circ$ and 15° respectively. For the angle of incidence $\gamma=0^\circ$, the DGA diagram was identical with the DGS diagram for the flat-bottomed reflector $D_{DSR}=2\text{mm}$ (Fig. 6, blue curve).

Each of the points making up a given DGA line expresses gain V determined for a specific beam path S for a given angle γ at which the beam strikes the reflector. On the basis of empirical points of previously described tests, linear approximation was used to obtain echo amplitude drop characteristics depending sole-

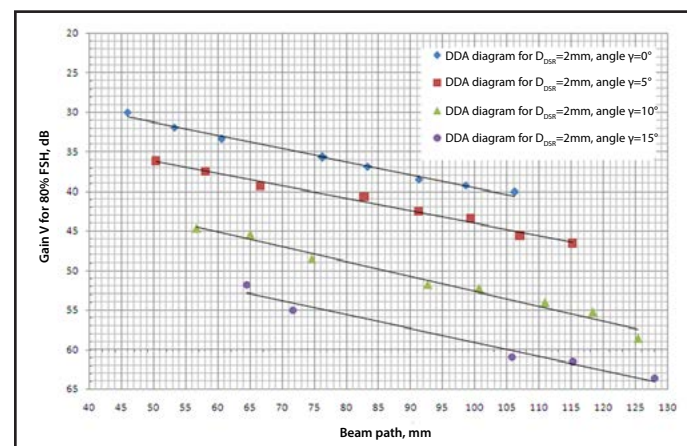


Fig. 6. Diagram “distance – gain - angle γ at which the beam strikes the reflector” for a circular flat-bottomed aperture of a diameter $D_{DSR}=2\text{mm}$ and angle γ values of $0^\circ, 5^\circ, 10^\circ$ and 15°

ly on angle γ . By reading the difference in gain between individual DGA lines for a given value of beam path S it is possible to obtain information about the echo amplitude decibel drop accompanying the change of a beam angle of incidence from 0° to $\gamma=5^\circ, 10^\circ$ or 15° . For instance, for a beam path $S=80\text{mm}$, a change in an angle of incidence from the optimum value ($\gamma=0^\circ$) to $\gamma=5^\circ$ is connected with an echo amplitude drop by approximately 5 dB; in turn, a change by 10° entails an amplitude drop of 13 dB, whereas a change by 15° results in a drop of almost 20 dB.

Irrespective of the beam path length S the amplitude drop characteristic is approximately repeatable for individual DGA lines, which

is demonstrated by the same distance between lines obtained for an increase in path length S . This indicates that the echo amplitude drop related to the change of angle γ does not depend on the beam path value. Obviously, this conclusion refers exclusively to the tested range of $S \approx 50 \div 120$ mm. However, this range was intentionally selected to include beam path values usually applied during tests of welded joints. Only for significant joint thicknesses the range of observation is greater than 120mm, yet its initial fragment ($0 \div 40$ mm) is rarely used.

Summary

The tests performed outline the problem of the course of amplitude echo changes accompanying the detection of unfavourably oriented flat discontinuities in ultrasonic tests of welded joints. The course is of great importance for assessments of flat discontinuities in conventional ultrasonic tests. When assessing indications in accordance with presently valid standard specifications [5], the primary criterion decisive for the acceptance of an indication is a decibel exceeding a related acceptance level, correlated with an appropriate reference level for the reference level adjustment technique according to PN-EN ISO 11666. As a result, in conventional ultrasonic tests, due to the lack of possibility related to beam insertion angle changes and because of the small selection of head angles, in the case of unfavourably oriented discontinuities the obtained decibel exceeding is significantly lower than the exceeding which could be obtained for the optimum angle at which the beam strikes the reflector, i.e. $\gamma = 0^\circ$. This effect results from the impossibility of adjusting the angle of beam insertion into the orientation of a given flat discontinuity. The presented diagrams of "distance – gain - beam angle of incidence on the reflector" represent the order of magnitude of an echo amplitude decibel drop accompanying the changes of angles at which the beam strikes a reflector by 5° , 10° and 15° .

In this respect, the use of ultrasonic tests of phased-array transducers enabling the obtainment of the optimum angle of incidence γ for most unfavourable orientations of discontinuities should increase their detectability and assessment accuracy. Such transducers enable the assessment of discontinuities for the beam insertion angle α at which an S-scan reveals the maximum echo amplitude, i.e. the amplitude where the angle at which the beam strikes a flat discontinuity is flat and amounts to $\gamma = 0^\circ$. However, a problem concerned with the use of the Phased Array method is the lack of standards specifying the assessment criteria when testing welded joints.

References

- [1] Kaczmarek R, Krawczyk R.: Badanie zmian amplitudy echa w zależności od kąta padania wiązki ultradźwiękowej na reflektor nieskończony. Biuletyn Instytutu Spawalnictwa, 2015, no. 3.
- [2] Kaczmarek R, Krawczyk R.: Analiza wpływu kąta ukosowania na wykrywalność przyklejeń brzegowych w ultradźwiękowej metodzie badań nieniszczących. Biuletyn Instytutu Spawalnictwa, 2014, no. 6.
- [3] Kaczmarek R, Krawczyk R.: Analiza wymiarów złączy próbných w procesie kwalifikowania technologii spawania wg PN-EN ISO 15614-1 w aspekcie badań ultradźwiękowych wg PN-EN ISO 17640. Biuletyn Instytutu Spawalnictwa, 2014, no. 4.
- [4] Kaczmarek R, Krawczyk R.: Projektowanie i wytwarzanie konstrukcji spawanych w aspekcie możliwości przeprowadzenia badań ultradźwiękowych wykonanych złączy. Przegląd Spawalnictwa, 2014, no. 7.
- [5] PN-EN ISO 11666: 2011: Non-destructive testing of welds – Ultrasonic testing – Acceptance levels